The inertial terms in equations of motion for bubbles in tubular vessels or between plates

T. G. Leighton[a)]
Institute of Sound and Vibration Research, University of Southampton, Highfield, Southampton SO17 1BJ, United Kingdom

(Received 29 June 2011; revised 18 August 2011; accepted 22 August 2011)

Equations resembling the Rayleigh-Plesset and Keller-Miksis equations are frequently used to model bubble dynamics in confined spaces, using the standard inertial term $R\ddot{R} + 3\dot{R}^2/2$, where R is the bubble radius. This practice has been widely assumed to be defensible if the bubble is much smaller than the radius of the confining vessel. This paper questions this assumption, and provides a simple rigid wall model for worst-case quantification of the effect on the inertial term of the specific confinement geometry. The relevance to a range of scenarios (including bubbles confined in microfluidic devices; or contained in test chambers for insonification or imaging; or in blood vessels) is discussed. © *2011 Acoustical Society of America*. [DOI: 10.1121/1.3638132]

PACS number(s): 43.35.Ei, 43.25.Yw, 43.80.Ev, 43.80.Qf [CCC] Pages: 3333–3338

I. INTRODUCTION

The increasing need to model nonlinear bubble pulsations within microfluidic devices and blood vessels has led to frequent use of the convenient Rayleigh-Plesset (RP)[1,2] or Keller-Miksis (KM)[3,4] equations. Although these equations sometimes include modifications to the terms that are traditionally placed on the right of the equation (e.g., to introduce additional damping or stiffness), the inertial term (the factor proportional to $R\ddot{R}+3\dot{R}^2/2$ which is traditionally on the left of the equation, where R is the bubble radius) is usually unmodified. Any justification for the use of $R\ddot{R}+3\dot{R}^2/2$ (or the equivalent volume frame term)[5] is usually limited to statements that it is allowed if the bubble radius R is always much less than the radius Γ_1 of the tube (or similar geometry, e.g., ink jet printer nozzle, microscope slide, etc.). Such an argument, unqualified, can never be correct because it does not refer to the length of the tube. Its continued use as a viable approximation should be subject to quantitative testing for the scenario in question. This paper provides a method for worst-case estimations by examining the effect of a simple rigid-wall model on the inertial term in the RP equation (extension to the KM equation is straightforward) for bubbles contained in tubes and between plates.

In this simple illustrative model for tubes, at ranges from the bubble center greater than roughly the tube radius Γ_1, the liquid is assumed to be lossless and to move in a one-dimensional[6] manner, contributing an inertial component that is proportional to the length of the tube. The effect on the inertia is obvious if the bubble fills the tube,[6,7] but it can also be significant if the bubble is much smaller than the tube radius,[8] depending on the length of the tube.[9–11]

Although the earliest studies emphasized the often dominant effect of the length of the tube on the inertia (both when the bubble is comparable with,[7,12] and when it is much smaller than,[8,9] the tube diameter), most subsequent studies of bubbles in tubes stated that unbounded models are a good approximation when the radius of the tube is much larger than the bubble, without qualifying this with a discussion of the tube length. Although the tube length was included explicitly in analyses of linear bubble pulsation,[6,7,13] the equivalent analysis for nonlinear[8,9] bubble pulsation has been adopted only rarely.[14] Scenarios of interest might include, for example, when *in vitro* data from contrast agents within tubular vessels are compared to predictions from RP/KM equations that have been comprehensively amended for the shell properties (or deformation of the bubble and vessel wall,[15–17] even with the vessel wall inertia included)[18] but retain unchanged the $R\ddot{R}+3\dot{R}^2/2$ inertial term (or its KM equivalent). The validity of this retention will depend on, say, the degree of acoustic transmission through the tube walls along their entire length,[19–27] which should be recorded. The next stage must be quantitatively to examine such standard inertial terms, and this paper transparently provides researchers who consider using RP/KM-type equations with a method of doing so that clearly attributes correction factors to the inertia of the various components of the system. It provides simple corrections to allow quick worst-case ("worst-case" in terms of having a rigid wall; if axial waves reflected back from the tube ends towards the bubble were not neglected, as here, greater discrepancies could occur) assessments as to whether unbounded results are applicable, providing modified inertia terms for RP equations should these be necessary. These could then be used as the foundation for inertial corrections which include end reflections and axial resonances, and wall compliance and flexibility.[28–30] The transparency of the inertial term allows explanation of the effects seen when tube length is varied.[31]

A similar analysis is conducted for bubbles between circular plates with rigid walls. The paper closes with a discussion of the relevance of these findings to microfluidic devices, *in vitro* tests and blood vessels.

a)Author to whom correspondence should be addressed. Electronic mail: tgl@soton.ac.uk

II. THEORY

A. The inertia of an unbounded spherical pulsating bubble

Consider a spherical gas bubble of radius R which changes volume but remains spherical in an infinite volume of incompressible liquid of density ρ_0 as a result of an insonifying field in the long wavelength limit. Conservation of mass implies

$$\rho_0 4\pi r^2(t)\dot{r}(t) = \rho_0 4\pi R^2(t)\dot{R}(t) \Rightarrow \dot{r} = \dot{R}R^2/r^2. \tag{1}$$

This is a trivial solution to the continuity equation in the incompressible limit, and shows that when the bubble wall moves with speed $\dot{R}$, the kinetic energy invested in the entire volume of the liquid (V_{liq}) is

$$\varphi_{\text{KE,sph}} = \frac{1}{2}\rho_0 \int_{V_{\text{liq}}} \dot{r}^2 \mathrm{d}V = \frac{1}{2}\rho_0 \int_{r=R}^{r=\infty} 4\pi r^2 \dot{r}^2 \mathrm{d}r$$
$$= \frac{1}{2}\left(4\pi\rho_0 R^3\right)\dot{R}^2 = \frac{1}{2}m_{\text{RF}}^{\text{rad}}\dot{R}^2. \tag{2}$$

If the inertia of the gas is assumed to make a negligible contribution, Eq. (2) indicates that the inertia (or "radiation mass") $m_{\text{RF}}^{\text{rad}} = 4\pi\rho_0 R^3$ associated with this wall motion is finite because the integral converges as a consequence of the inverse square fall-off of liquid velocity with distance from the bubble wall given by (1) (for small pulsations, $m_{\text{RF}}^{\text{rad}}$ is assumed to take a constant value $m_{\text{RF}}^{\text{rad}} = 4\pi\rho_0 R_0^3$ where R_0 is the equilibrium bubble radius, and RF indicates use of the radius-force frame since the expression varies between frames).[32] In two dimensions[33] (e.g., a bubble trapped between plates) the convergence is not so straightforward, and in one dimension the inertia never converges unless the tube length is finite.[6,7] The simple model of this paper assumes that such idealized fluid motions (neglecting turbulence, flow, transition zones, etc.) occur several vessel diameters away from the bubble. It gives worst-case predictions since the model assumes rigid walls, which some important practical scenarios do not possess (see Sec. III). This inertia enters the Rayleigh-Plesset equation because, as the bubble radius changes, kinetic energy is invested (primarily in the liquid) because of the difference between the work done remotely from the bubble by the liquid pressure far from the bubble $\{p_\infty = p_0 + P(t)$, which includes both static (p_0) and dynamic $[P(t)]$ components$\}$, and the work done by the pressure p_{L} at the bubble wall (ignoring hydrodynamic pressures etc. which may occur in confined flow). From Eq. (2) this energy balance is

$$\int_{r=R}^{r=\infty} (p_{\text{L}} - p_\infty) 4\pi R^2 \mathrm{d}R = 2\pi\rho_0 R^3 \dot{R}^2. \tag{3}$$

Differentiation of this with respect to R, noting that $\partial\dot{R}^2/\partial R = (\partial\dot{R}^2/\partial t)/\dot{R} = 2\ddot{R}$, gives

$$R\ddot{R} + 3\dot{R}^2/2 = \rho_0^{-1}[p_{\text{L}}(t) - p_0 - P(t)] + O(\dot{R}/c). \tag{4}$$

The term on the right in Eq. (4) arises from the difference in work done at the bubble wall and that done remotely from the bubble. The terms on the left arise from the kinetic energy imparted to the liquid and represent the inertia associated with the motion.

B. Inertia of a spherical pulsating bubble in a tube

If a spherical bubble changes volume in the middle of a rigid tube of radius Γ_1 and length $2\zeta_1$ where both the acoustic wavelength and ζ_1 are $\gg \Gamma_1 \gg R$ (Fig. 1), then a first order model (which ignores details of the transitional regime and the effect of reflected waves from the tube ends) can approximately subdivide[8] the liquid in the tube into two regions. In the first ($\Gamma_1 \gtrsim r > R$), the range r is measured from the center of the bubble, and the liquid motion is spherically symmetric. Further out from the bubble, and extending in both directions, the liquid motion is 1D, following the direction of the pipe axis, and range x is measured in this direction out from that pipe cross section which passes through the center of the bubble. The total kinetic energy $\phi_{\text{KE,tube}}$ invested in the liquid in the tube is assumed to be the sum of the kinetic energies of the liquid in both regions ($\varphi_{\text{KE,sph}}$ and $\varphi_{\text{KE,1D}}$, respectively). The total kinetic energy $\varphi_{\text{KE,Total\_1}}$ associated with bubble pulsation in the tube is therefore $\phi_{\text{KE,tube}}$ plus the kinetic energy invested with the inertia of the liquid associated with radiation of sound outside of the tube ends ($\varphi_{\text{KE,out}}$):

$$\varphi_{\text{KE,Total\_1}} = \varphi_{\text{KE,tube}} + \varphi_{\text{KE,out}}$$
$$= \varphi_{\text{KE,sph}} + \varphi_{\text{KE,1D}} + \varphi_{\text{KE,out}}. \tag{5}$$

The spherical component is approximately obtained by integrating Eq. (2) out to the tube radius Γ_1 using (1):

$$\varphi_{\text{KE,sph}} = \frac{1}{2}\rho_0 \int_{r=R}^{r=\Gamma_1} 4\pi r^2 \dot{r}^2 \mathrm{d}r = 2\pi\rho_0 \dot{R}^2 R^4 (R^{-1} - \Gamma_1^{-1})$$
$$= \frac{1}{2}\dot{R}^2\left[4\pi\rho_0 R^3 (1 - R/\Gamma_1)\right]. \tag{6}$$

The liquid in the tube at range x from the bubble wall where $\zeta_1 \gtrsim x \gtrsim \Gamma_1$, is assumed to move in 1D only with speed u_{1D}. Consequently the kinetic energy of the liquid that moves in

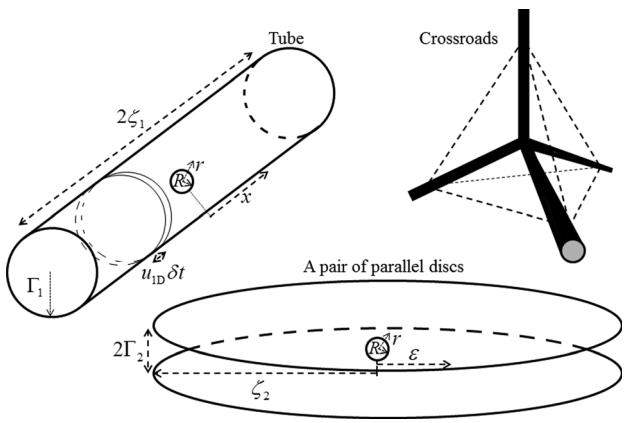

FIG. 1. Schematic showing the geometries discussed in this paper.

1D in the tube is found by integrating up the kinetic energy of disk-like fluid elements of area $\pi\Gamma_1^2$ and thickness dx in both directions away from the bubble (giving the factor of 2, below):

$$\varphi_{\mathrm{KE,1D}} = \frac{1}{2}\rho_0 2\int_{x=\Gamma_1}^{x=\zeta_1} \pi\Gamma_1^2 u_{1\mathrm{D}}^2 \mathrm{d}x = \frac{1}{2}\rho_0 2\pi\Gamma_1^2(\zeta_1-\Gamma_1)u_{1\mathrm{D}}^2. \quad (7)$$

In this first order calculation $u_{1\mathrm{D}}$ is found by matching the mass passing through cross-sections just before the two ends of the tube ($2\rho_0\pi\Gamma_1^2 u_{1\mathrm{D}}\delta t$; see Fig. 1) with the mass moving during the same time interval δt at the bubble wall ($\rho_0 4\pi R^2\dot{R}\delta t$). This implies that $u_{1\mathrm{D}} = 2R^2\dot{R}/\Gamma_1^2$ [recovery of Eq. (1) to resemble spherical spreading at $r=\Gamma_1$, but not beyond, would require that the bubble be placed at the center of a cross-roads where four identical tubes meet, e.g. in directions which map out the vertices of a regular tetrahedron; see Fig. 1]. Equations (6) and (7) therefore give

$$\varphi_{\mathrm{KE,tube}} = \varphi_{\mathrm{KE,sph}} + \varphi_{\mathrm{KE,1D}} = \frac{1}{2}\dot{R}^2\left\{\left[4\pi\rho_0 R^3(1-R/\Gamma_1)\right] + \left[8\pi\rho_0 R^4(\zeta_1-\Gamma_1)/\Gamma_1^2\right]\right\}, \quad (8)$$

where the inertia of the liquid contained within the tube is given by the term in curly {} brackets in Eq. (8). From Eq. (5) there is in addition inertia associated with the radiation of sound out of the ends of the tube. This might be due to tube branching, opening into some larger vessel, or represent radiation from both ends of the tube into unbounded liquid. Taking the specific example where the tube is cut into a rigid planar block such that both ends of the tube radiate from a baffled opening in the block out into a semi-infinite half-space in the manner described by Ref. 34, the extra inertia can be accounted for[34,35] by adding a virtual length $8\Gamma_1/(3\pi)$ to the tube in both directions. Consequently the total inertia associated with such assumed bubble pulsation in a rigid tube which radiates to free space at both baffled ends is

$$m_1 = 4\pi\rho_0 R^3\left(1-\frac{R}{\Gamma_1}\right) + \frac{8\pi\rho_0 R^4}{\Gamma_1}\left(\frac{\zeta_1}{\Gamma_1}\left[1+\frac{8}{3\pi}\frac{\Gamma_1}{\zeta_1}\right]-1\right). \quad (9)$$

Most of the above inertial contributions do not depend on tube length ζ_1. These include the first term (the inertia of the liquid close to the bubble, the subtraction of R/Γ_1 indicating that the spherical symmetry is limited to within about one tube radius of the bubble wall); the $8/(3\pi)$ associated with radiation out of the tube ends; and the "-1" component of the second term (i.e., the subtraction that must occur because not all of the liquid in the tube—specifically the liquid within about one tube radius of the bubble—moves in a 1D manner). The remaining inertia (the first unity in the second term) represents the inertia of the liquid moving in 1D. It contains $(R/\Gamma_1)^2$ and it might be the presence of this ratio which led to the misleading statements that the effect of the tube can be ignored if the radius of the bubble is much less than that of the tube. This term is multiplied by ζ_1, and so increases monotonically with tube length, which will eventually outweigh the smallness of $(R/\Gamma_1)^2$ for long non-branching tubes of constant cross section.

This rigid-wall worst-case formulation can be used to quantify the magnitude of the discrepancy of the real inertia from that assumed for an infinite volume of liquid. Dividing Eq. (9) by $m_{\mathrm{RF}}^{\mathrm{rad}} = 4\pi\rho_0 R^3$ from (2) gives

$$m_1/m_{\mathrm{RF}}^{\mathrm{rad}} \approx \left(1-\frac{R}{\Gamma_1}\right) + \frac{2R}{\Gamma_1}\left\{\frac{\zeta_1}{\Gamma_1}\left[1+\frac{8}{3\pi}\frac{\Gamma_1}{\zeta_1}\right]-1\right\}. \quad (10)$$

To recap, the first term (in round brackets) arises from the inertia close to the bubble wall ($\Gamma_1 > r > R$) where the $(-R/\Gamma_1)$ is proportional to the inertia subtracted away because the spherical symmetry does not extend to infinity. This subtraction can find approximate compensation by the addition to the second bracketed term of $8/(3\pi)$ which arises from the radiation into two half spaces that is assumed here to occur outside of the ends of the tube. This term would change if the radiation out of the tube ends was into some other form of space.[36] In the baffled case assumed for (10), it has value $[16/(3\pi)](R/\Gamma_1) \approx 1.7(R/\Gamma_1)$, the rigid baffles overcompensating as expected for the R/Γ_1 subtracted from the first term.

Table I plots $m_1/m_{\mathrm{RF}}^{\mathrm{rad}}$ as a function of the half-length of the tube (normalized to its radius), ζ_1/Γ_1, for a bubble of 2 μm radius. The second column shows the multiplicative factor by which the tube length must be increased to account for the assumed radiation out of the two baffled ends of the tube into the half-space. This is not a function of the bubble size and decreases as the real tube length increases. The departure of $m_1/m_{\mathrm{RF}}^{\mathrm{rad}}$ from the value of unity that it would take were the bubble not contained in a tube, increases with decreasing tube radius and increasing tube length.

Although the modeled geometry reduces the effect of the standard $R\ddot{R}+3\dot{R}^2/2$ term in the Rayleigh-Plesset equation (by removing the inertia of the spherically spreading liquid further from the bubble than about one

TABLE I. The ratio of the inertia calculated from Eq. (9) to that assumed in the standard Rayleigh-Plesset formulation for a bubble of 2 μm radius in rigid-walled tubes of the radii and lengths shown.

Proportional half-length of tube (ζ_1/Γ_1)	Normalized end-correction $\frac{8}{3\pi}\frac{\Gamma_1}{\zeta_1}$	$m_1/m_{\mathrm{RF}}^{\mathrm{rad}}$ for a tube of radius: $\Gamma_1 = 1$ mm	$\Gamma_1 = 0.1$ mm	$\Gamma_1 = 20$ μm
5	0.1698	1.02	1.17	1.87
10	0.0849	1.04	1.37	2.87
20	0.0424	1.08	1.77	4.87
50	0.0170	1.20	2.97	10.87
100	0.0085	1.40	4.97	20.87
200	0.0042	1.80	8.97	40.87
500	0.0017	3.00	20.97	100.87
1000	0.0008	5.00	40.97	200.87

tube radius), this will be approximately compensated by the radiation out of the ends of the tube. More importantly, the rigid wall tube geometry and fluid motion assumed here will add a new term associated with the liquid that moves in 1D along the vessel. For the tube model assumed here, the assumption that the Rayleigh-Plesset inertial term of $R\ddot{R}+3\dot{R}^2/2$ is appropriate is therefore never strictly correct, although the limits of applicability for those models can be assessed using worst-case estimations (Table I) or the RP/KM equations can be adapted for such inertial effects. The appropriate RP equations consistent with this model (a central bubble between rigid walls, with radiation out into half-spaces via baffled exits at the tube extremities) can be found by equating the work done on the bubble gas with the kinetic energy in the liquid:

$$\begin{aligned}\int_{r=R}^{r=\infty}(p_{\mathrm{L}}-p_\infty)4\pi R^2\mathrm{d}R &= \varphi_{\mathrm{KE,tot}}=\frac{1}{2}\dot{R}^2\left\{4\pi\rho_0R^3\left(1-\frac{R}{\Gamma_1}\right)\right.\\ &\left.+\frac{8\pi\rho_0R^4}{\Gamma_1}\left(\frac{\zeta_1}{\Gamma_1}\left[1+\frac{8}{3\pi}\frac{\Gamma_1}{\zeta_1}\right]-1\right)\right\},\end{aligned}\tag{11}$$

the term in curly brackets {} being the inertia as taken from (9). Differentiation of this with respect to R gives

$$\begin{aligned}&R\ddot{R}\left[1+\frac{R}{\Gamma_1}\left\{2\left(\frac{\zeta_1}{\Gamma_1}\left[1+\frac{8}{3\pi}\frac{\Gamma_1}{\zeta_1}\right]-1\right)-1\right\}\right]\\ &+\frac{3}{2}\dot{R}^2\left[1+\frac{4R}{3\Gamma_1}\left\{2\left(\frac{\zeta_1}{\Gamma_1}\left[1+\frac{8}{3\pi}\frac{\Gamma_1}{\zeta_1}\right]-1\right)-1\right\}\right]\\ &=\frac{1}{\rho_0}(p_{\mathrm{L}}(t)-p_0-P(t))+O(\dot{R}/c).\end{aligned}\tag{12}$$

In each of the square brackets, the first unity term is from the standard RP equation term $(R\ddot{R}+3\dot{R}^2/2)$ for spherical symmetry from the bubble wall out to infinity. The fourth unity term in each square bracket arises from the "lost" inertia that must be subtracted because the spherical symmetry does not extend to infinity. The second unity term in each square bracket arises from the liquid moving in 1D in the tube [noting that departure in radiation conditions outside of the tube from those assumed here will require a change to the end-correction $(\Gamma_1/\zeta_1)8/(3\pi)$]. The third unity term in each square bracket arises from the fact that the liquid close to the bubble wall does not undergo 1D motion and so a term must be subtracted from the inertia associated with 1D motion in the tube.

C. Inertia of a spherical pulsating bubble between disks

A 2D equivalent of this simple formulation (with the same limiting assumptions) considers a central bubble between two rigid disks of radius ζ_2 separated by $2\Gamma_2$ (Fig. 1). At the extreme of the disks there is radiation into some outer environment (which might be constrained or unconstrained). The fluid motion between the disks is subdivided into a spherically spreading region from the bubble wall to range $r\approx\Gamma_2$ beyond which transition region the particle velocity $\dot{\varepsilon}$ and range ε measurements are normal to the axis of symmetry that passes through the center of the bubble and the disks. If the liquid is incompressible then in time δt the mass $\rho_0 4\pi\varepsilon\Gamma_2\dot{\varepsilon}\delta t$ of liquid passing through a cylindrical control surface in this regime equals the mass $\rho_0 4\pi R^2\dot{R}\delta t$ passing through a spherical control surface at the bubble wall, from which equality $\dot{\varepsilon}=\dot{R}R^2/(\varepsilon\Gamma_2)$. This can be used to obtain the kinetic energy of the axisymmetric motion:

$$\begin{aligned}\varphi_{\mathrm{KE,2D}}&=\frac{1}{2}\rho_0 2\Gamma_2\int_{\varepsilon=\Gamma_2}^{\varepsilon=\zeta_2^*}2\pi\varepsilon\dot{\varepsilon}^2\mathrm{d}\varepsilon\\ &=\frac{1}{2}\rho_0 2\Gamma_2\int_{\varepsilon=\Gamma_2}^{\varepsilon=\zeta_2^*}2\pi\varepsilon\left(\frac{\dot{R}R^2}{\varepsilon\Gamma_2}\right)^2\mathrm{d}\varepsilon\\ &=\left(\frac{\dot{R}^2}{2}\right)\frac{4\pi\rho_0R^4}{\Gamma_2}\ln\left(\frac{\zeta_2^*}{\Gamma_2}\right),\end{aligned}\tag{13}$$

where ζ_2^* represents the artificially enhanced disk radius that also accounts for the inertia associated with the liquid motion outside of the disks. Combining this with the spherical inertia resembling (6) gives a total inertia of $m_2\approx 4\pi\rho_0R^3\left[(1-R/\Gamma_2)+(R/\Gamma_2)\ln(\zeta_2^*/\Gamma_2)\right]$, so that the ratio $m_2/m_{\mathrm{RF}}^{\mathrm{rad}}$ is $(1-R/\Gamma_2)+(R/\Gamma_2)\ln(\zeta_2^*/\Gamma_2)$. In this, the first R/Γ_2 is proportional to the inertia subtracted away from $m_{\mathrm{RF}}^{\mathrm{rad}}$ because the spherical symmetry does not extend to infinity, and the $R/\Gamma_2\ln(\zeta_2^*/\Gamma_2)$ is proportional to the inertia in the axisymmetric section (the Γ_2 in the natural log accounting for the absence of 2D motion in the region $\Gamma_2>r>R$ where spherical motion occurs). Note that ζ_2^*, the enhanced version of ζ_2, is being used to include the inertia of the liquid outside of the disks. For a bubble of radius 2 μm placed centrally between two 1-cm radius coins spaced 100 μm apart, $m_2/m_{\mathrm{RF}}^{\mathrm{rad}}$ equals $\sim$1.17, the discrepancy as expected being less than that when the bubble is confined in a tube because of the fall-off of particle velocity with range. From Eq. (13) the equivalent energy balance to Eq. (11) for this coin-confined geometry[37] (resembling some *in vitro* arrangements, resonant chamber bubble detectors, microfluidic devices, microscope wells and sonic traps) is

$$\begin{aligned}\int(p_{\mathrm{L}}-p_\infty)4\pi R^2\mathrm{d}R &= \varphi_{\mathrm{KE,tot}}=\frac{1}{2}\dot{R}^2m_2\\ &\approx 2\pi\rho_0\left[R^3\dot{R}^2-\frac{R^4\dot{R}^2}{\Gamma_2}\left(1-\ln\frac{\zeta_2^*}{\Gamma_2}\right)\right].\end{aligned}\tag{14}$$

Differentiation of this with respect to R gives

$$\begin{aligned}&R\ddot{R}\left[1+\frac{R}{\Gamma_2}\left(\ln\frac{\zeta_2^*}{\Gamma_2}-1\right)\right]\\ &+\frac{3}{2}\dot{R}^2\left[1+\frac{4R}{3\Gamma_2}\left(\ln\frac{\zeta_2^*}{\Gamma_2}-1\right)\right]\\ &=\frac{1}{\rho_0}[p_{\mathrm{L}}(t)-p_0-P(t)]+O(\dot{R}/c)\end{aligned}\tag{15}$$

the additions and subtractions from the standard RP equation being transparent in a manner that is similar to the

description after Eq. (12). As with bubble pulsation in a tube, volume changes in bubbles close to plates (and other bubbles) can induce loss of sphericity,[38–45] and Klaseboer and Khoo[46] indicated how these, and other real-word effects, might be incorporated into an RP-like formulation.

III. DISCUSSION

When bubbles pulsate in real vessels, there will be departures to a greater or lesser extent from the rigid wall boundary conditions and assumed 1D/2D particle velocities (with simple transition zones between these and the spherical conditions near the bubble) that are inherent in the preceding theory. Hence the above formulations provide a way of making worst-case estimates of the effect of the enhanced inertia: if such calculations show negligible effect then standard inertial terms can be used, but if not the implications need to be considered. Enhancement of the inertia could affect the measurement or exploitation of the bubble dynamics and resonance in a microfluidic device,[47,48] or in a chamber or Petri dish for cell treatment,[49,50] or in a glass/plastic capillary tube, or in a chamber on a microscope slide. This will reduce the resonance frequency of the, contrast agent[6,7] (confinement can also affect the damping)[51,52], with commensurate implications for fitting parameters to free field models to match data obtained from confined bubbles. If the $R\ddot{R}+3\dot{R}^2/2$ terms do need to be amended, this will affect not only the bubble dynamics but also the predictions of scattered pressure for confined bubbles,[19,22,53] since this depends on such terms.[32] In the limit of long vessels, the inertia becomes huge, so that the vessel (not the liquid column) provides the compliance for bubble growth.[6,7,25,54] This hydrodynamic constraint will also be important for large bubbles in terms of loss of sphericity.[15,18,55]

Blood vessels depart significantly from the conditions assumed by the theory. Blood vessels will branch, although a pairwise branching into identical daughter vessels will only double the area with distance, which provides less spreading loss than the inverse square law associated with spherical spreading. More importantly, blood vessel walls are compliant, and (unless next to gas or bone) they readily transmit sound from within the blood out into the surrounding tissue, which will incur commensurate spreading losses, and absorption will also occur. As such, the above theory can only be used with *in vivo* blood vessels for the worst-case estimations described above, or as the basis for the development of a more complete theory specifically for such vessels.

With the increasing attention paid to measurements of confined bubbles, these worst-case calculations allow assessment to be made as to whether the left (inertial) sides of the RP and KM equations require attention to complement the work to date that has focused on amending the right (stiffness, elasticity and damping) sides of these equations. The bulk of bubble dynamics is based on stationary bubbles in the free field, e.g., through simplification of the Navier-Stokes equation and boundary conditions. Other areas where use of established theory could be critically assessed for their applicability to bubbles within vessels containing flowing viscous liquids, are neglect of the convective terms; neglect of the vector summation of all body forces; neglect of the term $\bar{\nabla}\times\bar{\nabla}\times\bar{u}$ which encompasses the dissipation of acoustic energy associated with, amongst other things, vorticity; and (perhaps most immediately given that the dynamics of contrast agents in compressible liquids are now being simulated) the terms associated with the bulk viscosity.[56]

IV. CONCLUSIONS

The statement that the use of the standard $R\ddot{R}+3\dot{R}^2/2$ inertial term in the RP equation is justified for bubbles contained in a tube if the bubble is much smaller than the vessel diameter can never be correct, since it makes no mention of the tube length. The size of the discrepancy will depend on the transmissivity and compliance of the walls, the tube geometry, and details of the particle velocity both inside and outside of the tube. Whether this is important for a given scenario can be assessed using the simple rigid-walled model to give a worst-case estimate of the effect on the inertia. It is directly applicable to some circumstances (bubbles within thick-walled steel tubes) and would provide the foundation for more sophisticated models of bubbles contained within compliant walls with detailed transition zones. Future work will consider the effect of the key assumptions, and indeed greater discrepancies than are forecast by the "worst case" model of this paper may be predicted when the effect on the bubble of reflections from the tube boundaries, and the occurrence of axial resonances, are included.

[1]H. G. Flynn, "Physics of acoustic cavitation in liquids," in *Physical Acoustics*, edited by W. P. Mason (Academic, New York, 1964), Vol. 1, Part B, pp. 58–172.
[2]M. S. Plesset and A. Prosperetti, "Bubble dynamics and cavitation," Annu. Rev. Fluid Mech. **9**, 145–185 (1977).
[3]J. B. Keller and M. Miksis, "Bubble oscillations of large amplitude," J. Acoust. Soc. Am. **68**, 628–633 (1980).
[4]A. Prosperetti, L. A. Crum, and K. W. Commander, "Nonlinear bubble dynamics," J. Acoust. Soc. Am. **83**, 502–514 (1988).
[4]T. G. Leighton, "The Rayleigh-Plesset equation in terms of volume with explicit shear losses," Ultrasonics **48**(2), 85–90 (2008).
[6]T. G. Leighton, P. R. White, and M. A. Marsden, "Applications of one-dimensional bubbles to lithotripsy, and to diver response to low frequency sound," Acta Acust. **3**, 517–529 (1995).
[7]T. G. Leighton, P. R. White, and M. A. Marsden, "The one-dimensional bubble: An unusual oscillator, with applications to human bioeffects of underwater sound," Eur. J. Phys. **16**, 275–281 (1995).
[8]T. G. Leighton, A. D. Phelps, B. T. Cox, and W. L. Ho, "Theory and preliminary measurements of the Rayleigh-like collapse of a conical bubble," Acta Acust. **84**, 1014–1024 (1998).
[9]T. G. Leighton, B. T. Cox, and A. D. Phelps, "The Rayleigh-like collapse of a conical bubble," J. Acoust. Soc. Am. **107**, 130–142 (2000).
[10]T. G. Leighton, B. T. Cox, P. R. Birkin, and T. Bayliss, "The Rayleigh-like collapse of a conical bubble: Measurements of meniscus, liquid pressure, and electrochemistry," in *Proceedings of the 137th Regular Meeting of the Acoustical Society of America and the 2nd Convention of the European Acoustics Association (Forum Acusticum 99, integrating the 25th German Acoustics DAGA Conference)*, Paper 3APAB_1 (March 1999).
[11]T. G. Leighton, W. L. Ho, and R. Flaxman, "Sonoluminescence from the unstable collapse of a conical bubble," Ultrasonics **35**, 399–405 (1997).
[12]N. W. Jang, S. M. Gracewski, B. Abrahamsen, T. Buttaccio, R. Halm, and D. Dalecki, "Natural frequency of a gas bubble in a tube: Experimental and simulation results," J. Acoust. Soc. Am. **126**, EL34–EL40 (2009).
[13]H. N. Oguz and A. Prosperetti, "The natural frequency of oscillation of gas bubbles in tubes," J. Acoust. Soc. Am. **103**, 3301–3308 (1998).
[14]E. Sassaroli and K. Hynynen, "Cavitation threshold of microbubbles in gel tunnels by focused ultrasound," Ultrasound Med. Biol. **33**, 1651–1660 (2007).

[15]Y. T. Hu, S. Qin, T. Hu, K. W. Ferrara, and Q. Jiang, "Asymmetric oscillation of cavitation bubbles in a microvessel and its implications upon mechanisms of clinical vessel injury in shock-wave lithotripsy," Int. J. Non-Linear Mech. **40**, 341–350 (2005).
[16]S. Qin, Y. Hu, and Q. Jiang, "Oscillatory interaction between bubbles and confining microvessels and its implications on clinical vascular injuries of shock-wave lithotripsy," IEEE Trans. Ultrason. Ferroelectr. Freq. Control **53**, 1322–1329 (2006).
[17]E. P. Stride and C. C. Coussios, "Cavitation and contrast: The use of bubbles in ultrasound imaging and therapy," Proc. Inst. Mech. Eng. Part H: J. Eng. Med. **224**, 171–191 (2010).
[18]F. Gao, Y. Hu, and H. Hu "Asymmetrical oscillation of a bubble confined inside a micro pseudoelastic blood vessel and the corresponding vessel wall stresses," Int. J. Solids Struct. **44**, 7197–7212 (2007).
[19]P. A. Dayton, J. E. Chomas, A. F. H. Lum, J. S. Allen, J. R. Lindner, S. I. Simon, and K. W. Ferrara, "Optical and acoustical dynamics of microbubble contrast agents inside neutrophils," Biophys. J. **80**, 1547–1556 (2001).
[20]P. Marmottant, S. van der Meer, M. Emmer, M. Versluis, N. de Jong, S. Hilgenfeldt, and D. Lohse, "A model for large amplitude oscillations of coated bubbles accounting for buckling and rupture," J. Acoust. Soc. Am. **118**, 3499–3505 (2005).
[21]C. F. Caskey, D. E. Kruse, P. A. Dayton, T. K. Kitano, and K. W. Ferrara, "Microbubble oscillation in tubes with diameters of 12, 25, and 195 microns," Appl. Phys. Lett. **88**, 033902 (2006).
[22]J. Sijl, E. Gaud, P. J. A. Frinking, M. Arditi, N. de Jong, D. Lohse, and M. Versluis, "Acoustic characterization of single ultrasound contrast agent microbubbles," J. Acoust. Soc. Am. **124**, 4091–4097 (2008).
[23]P. A. Dayton, J. S. Allen and K. W. Ferrara, "The magnitude of radiation force on ultrasound contrast agents," J. Acoust. Soc. Am. **112**, 2183–2192 (2002).
[24]J. P. Kilroy, A. V. Patil, and J. A. Hossack, "Ultrasound Catheter for microbubble based drug delivery," Ultrasonics Symposium (IUS), 2009 IEEE International (Rome, Italy), IEEE Ultrasonics Symposium, 2770–2773 (2009), doi:2009.5442089.
[25]J. B. Freund, "Suppression of shocked bubble expansion due to tissue confinement with application to shock wave lithotripsy," J. Acoust. Soc. Am. **123**, 2867–2874 (2008).
[26]T. Gehrke and H. M. Overhoff, "Simulation of contrast agent enhanced ultrasound imaging based on Field II, Bildverarbeitung für die Medizin 2008, Algorithmen — Systeme — Anwendungen Proceedings des Workshops vom 6. bis 8. April 2008, Berlin (Springer, Berlin, 2008), p. 62–66.
[27]A. D. Mansfel'd, D. A. Mansfel'd, and A. M. Reĭman, "Abilities of nonlinear acoustic methods in locating gas bubbles in biological tissues," Acoust. Phys. **51**, 209–217 (2005). Translated from Akusticheskiĭ Zhurnal **51**, 259–267 (2005).
[28]T. Ye and J. L. Bull, "Microbubble expansion in a flexible tube," J. Biomech. Eng. **128**, 554–563 (2006).
[29]S. Qin and K.W. Ferrara, "Acoustic response of compliable microvessels containing ultrasound contrast agents," Phys. Med. Biol. **51**, 5065–5088 (2006).
[30]S. Qin and K.W. Ferrara, "The natural frequency of nonlinear oscillation of ultrasound contrast agents in microvessels," Ultrasound Med. Biol. **33**, 1140–1148 (2007).
[31]H. Miao, S. M. Gracewski, and D. Dalecki, "Ultrasonic excitation of a bubble inside a deformable tube: Implications for ultrasonically induced hemorrhage," J. Acoust. Soc. Am. **124**, 2374–2384 (2008).
[32]T. G. Leighton, *The Acoustic Bubble* (Academic Press, London, 1994), pp. 93–101, 140–141, 151–153.
[33]T. G. Leighton, P. R. White, and M. F. Schneider, "The detection and dimension of bubble entrainment and comminution," J. Acoust. Soc. Am. **103**, 1825–1835 (1998).
[34]D. T. Blackstock, *Fundamentals of Physical Acoustics* (Wiley, New York, 2000), pp. 144–163.
[35]T. G. Leighton, "Fluid loading effects for acoustical sensors in the atmospheres of Mars, Venus, Titan and Jupiter," J. Acoust. Soc. Am. **125**(5), EL214–EL219 (2009).
[36]P. M. Morse and K. U. Ingard, *Theoretical Acoustics* (Princeton University Press, Princeton, New Jersey, 1968), pp. 467–477.
[37]J. Cui, M. F. Hamilton, P. S. Wilson, and E. A. Zabolotskaya, "Bubble pulsations between parallel plates," J. Acoust. Soc. Am. **119**, 2067–2072 (2006).
[38]T. B. Benjamin and A. T. Ellis, "Collapse of cavitation bubbles and pressure thereby produced against solid boundaries," Philos. Trans. R. Soc. London A **260**, 221–240 (1966).
[39]A. Shima and K. Nakajima, "Collapse of a non-hemispherical bubble attached to a solid wall," J. Fluid Mech. **80**, 369–391 (1977).
[40]J. R. Blake and D. C. Gibson, "Cavitation bubbles near boundaries," Annu. Rev. Fluid Mech. **19**, 99–123 (1987).
[41]O. Lindau and W. Lauterborn, "Cinematographic observation of the collapse and rebound of a laser-produced cavitation bubble near a wall," J. Fluid Mech. **479**, 327–348 (2003).
[42]C. K. Turangan, A. R. Jamaluddin, G. J. Ball, and T. G. Leighton, "Free-Lagrange simulations of the expansion and jetting collapse of air bubbles in water," J. Fluid Mech. **598**, 1–25 (2008).
[43]K. Y. Lim, P. A. Quinto-Su, E. Klaseboer, B. C. Khoo, V. Venugopalan, and C. D. Ohl, "Nonspherical laser-induced cavitation bubbles," Phys. Rev. E **81**, 016308 (2010).
[44]A. R. Jamaluddin, G. J. Ball, C. K. Turangan, and T. G. Leighton, "The collapse of single bubbles and calculation of the far-field acoustic emissions for cavitation induced by shock wave lithotripsy," J. Fluid Mech. **677**, 305–341 (2011).
[45]S. R. Gonzalez-Avila, E. Klaseboer, B. C. Khoo, and C. D. Ohl, "Cavitation bubble dynamics in a liquid gap of variable height," J. Fluid Mech. **682**, 241–260 (2011).
[46]E. Klaseboer and B. C. Khoo, "A modified Rayleigh-Plesset model for a non-spherically symmetric oscillating bubble with applications to boundary element methods," Eng. Anal. Boundary Elem. **30**, 59–71 (2006).
[47]S. Le Gac, E. Zwaan, A. Van Den Berg, and C. D. Ohl, "Sonoporation of suspension cells with a single cavitation bubble in a microfluidic confinement," Lab Chip **7**, 1666–1672 (2007).
[48]P. A. Quinto-Su, K. Y. Lim, and C. D. Ohl, "Cavitation bubble dynamics in microfluidic gaps of variable height," Phys. Rev. E **80**, 047301 (2009).
[49]M. J. W. Pickworth, P. P. Dendy, P. R. Twentyman, and T. G. Leighton, "Studies of the cavitational effects of clinical ultrasound by sonoluminescence: 4. The effect of therapeutic ultrasound on cells in monolayer culture in a standing wave field," Phys. Med. Biol. **34**(11), 1553–1560 (1989).
[50]C. D. Ohl, M. Arora, R. Ikink, N. de Jong, M. Versluis, M. Delius, and D. Lohse, "Sonoporation from jetting cavitation bubbles," Biophys. J. **91**, 4285–4295 (2006).
[51]T. G. Leighton, P. R. White, C. L. Morfey, J. W. L. Clarke, G. J. Heald, H. A. Dumbrell, and K. R. Holland, "The effect of reverberation on the damping of bubbles," J. Acoust. Soc. Am. **112**, 1366–1376 (2002).
[52]T. G. Leighton., D. G. Ramble, A. D. Phelps, C. L. Morfey, and P. P. Harris, "Acoustic detection of gas bubbles in a pipe," Acust. Acta Acust. **84**, 801–814 (1998).
[53]A. A. Doinikov, L. Aired and A. Bouakaz, "Acoustic response from a bubble pulsating near a fluid layer of finite density and thickness," J. Acoust. Soc. Am. **129**, 616–621 (2011).
[54]S. Martynov, E. Stride and N. Saffari, "The natural frequencies of microbubble oscillation in elastic vessels," J. Acoust. Soc. Am. **126**, 2963–2972 (2009).
[55]J. B. Freund, R. K. Shukla and A. P. Evan, "Shock-induced bubble jetting into a viscous fluid with application to tissue injury in shock-wave lithotripsy," J. Acoust. Soc. Am. **126**, 2746–2756 (2009).
[56]M. A. Ainslie and T. G. Leighton, "Review of scattering and extinction cross-sections, damping factors, and resonance frequencies of a spherical gas bubble," J. Acoust. Soc. Am. (in press).